Langmuir

ARTICLE

pubs.acs.org/Langmuir

Wettability Conversion from Superoleophobic to Superhydrophilic on Titania/Single-Walled Carbon Nanotube Composite Coatings

Min Zhang, Tao Zhang, and Tianhong Cui*

Department of Mechanical Engineering, University of Minnesota, Minneapolis, Minnesota 55455, United States

Supporting Information

ABSTRACT: Superoleophobic surfaces were demonstrated on perfluorosilane-rendered titania (TiO_2)/single-walled carbon nanotube (SWNT) composite coatings. Scanning electron microscopy (SEM) and transmission electron microscopy (TEM) observations revealed that SWNTs play a key role in the formation of overhanging structures and the nanoscale roughness on the coating surface, which compose the two critical morphologic factors for a superoleophobic surface. The wettability conversion from superoleophobic to superhydrophilic of the composite coatings was realized by the gradual decomposition of 1*H*,1*H*,2*H*,2*H*-perfluorodecyltrichlorosilane (FDTS) on the coating surface using UV irradiation. Contact angle measurement on both smooth TiO_2 surface and rough composite coating surface under different UV irradiation time revealed that the wetting behavior of the liquids on the composite coating surface passes from the Cassie to the Wenzel and finally to the inversed-Cassie regime. Different liquids show different irradiation time for the wetting state change. By controlling the UV irradiation dose, liquids with surface tension difference smaller than 5 mN/m can exist in completely converse wetting states on the same coating surface, that is, superphobic for one liquid while superphilic for another with lower surface tension. Mixed organic liquids with different surface tension can be completely separated through a coated grid using this wettability tuning technique.

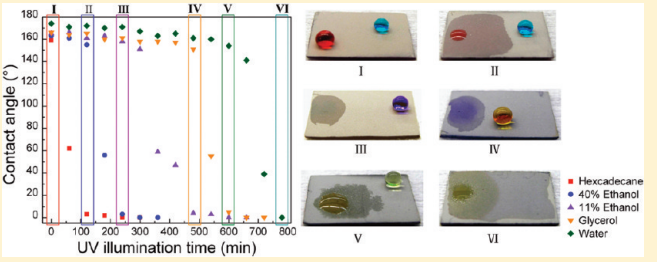

1. INTRODUCTION

Surfaces with extreme wetting states, superhydrophobicity and superhydrophilicity, exist extensively in nature and allow biospecies to adapt themselves to their surrounding environment.[1−3] Recognizing the roles of the two key parameters, surface energy and roughness, of these surfaces has led to the development of plenty of artificial superhydrophobic and superhydrophilic materials.[4−10] The reversible conversion between superhydrophobic and superhydrophilic states on these materials can be achieved by tuning the surface energy using various types of stimuli, including light,[6] heat,[7] electrical field,[8] or surfactant.[9] However, the conversion of the two extreme wetting states for liquids with lower surface tension than water (surface tension γ_{lv} = 72.1 mN/m), such as glycerol (γ_{lv} = 63.0 mN/m) or hexadecane (γ_{lv} = 27.6 mN/m), has seldom been achieved because creating superphobic surfaces to such liquids is much more difficult than creating superhydrophobic surfaces. Recently, superoleophobic surfaces, that is, surfaces with super-repellent properties to low-surface-tension liquids, have been realized by several researchers.[11−17] Such achievements open a door to the modulation of the surface wettability for various liquids with surface tension between oil and water.

Thanks to the photocatalytic and photostimulated superhydrophilic properties, titania (TiO_2) allows the superhydrophobic−superhydrophilic conversion on the same surface by modifying the TiO_2 surface with a hydrophobic self-assembled monolayer and UV irradiation alternately.[6,10,18] Superoleophobic TiO_2 surfaces, however, have seldom been obtained probably due to the difficulty of fabricating overhanging TiO_2 structures on which a liquid can exist in Cassie−Baxter state (henceforth the Cassie state),[19] which proved to be a critical factor of the superoleophobic surface.[11]

In the present work, we demonstrate that superoleophobic surface can be obtained on perfluorosilane-rendered TiO_2/single-walled carbon nanotube (SWNT) composite coatings. Through ultraviolet (UV) irradiation, the wettability of such coating can be tuned from superoleophobic to superhydrophilic. During this conversion, the coating surface can be modulated from superphobic to superphilic for any liquids we used with surface tension between 27 mN/m (hexadecane) and 72 mN/m (water). Moreover, by controlling the dose of the UV irradiation, superphobicity and superphilicity can exist on the same coating surface for liquids with different surface tensions, including various organic liquids and water.

2. EXPERIMENTAL SECTION

2.1. Synthesis and Surface Modification of TiO_2/SWNT Composite Coatings. Liquid phase deposition (LPD) is a wet process for the synthesis of metal oxide thin films.[20,21] Here, a modified LPD process, composite LPD (c-LPD), was used to synthesize the

Received: January 30, 2011
Revised: April 8, 2011
Published: July 06, 2011

TiO_2/SWNT composite coatings. In this process, SWNTs were introduced in the reaction solution as a second phase to modify the morphology of the TiO_2 coatings. As the parent solutions for deposition, ammonium hexafluorotitanate ($(NH4)_2TiF_6$) (Sigma-Aldrich Co.) and boric acid (H_3BO_3) (Sigma-Aldrich Co.) were dissolved in deionized water at a concentration of 0.3 and 0.4 M, respectively. After the two solutions were mixed together, 1−4 μg/mL 99% purified single-walled carbon nanotube (SWNT) (Nanointegris, U.S.) was dispersed in the solution by ultrasonic treatment for 5 min. Silicon wafer substrates cleaned by standard Piranha etching solution were immersed into the treatment solution and stayed at the bottom horizontally at 45 °C for 12 h. Next, the substrates were removed from the solution, rinsed with a copious amount of deionized water, and dried in a nitrogen stream. TiO_2 film was synthesized as a result of the following hydrolysis reaction:[22]

$$(NH_4)_2TiF_6 + 2H_2O = TiO_2 + 2NH_4F + 4HF$$

The addition of H_3BO_3 shifts the equilibrium of this reaction to the right due to a consumption reaction with F according to the following equation:

$$H_3BO_3 + 4HF = BF_4 + H_3O^+ + 2H_2O$$

The freshly prepared TiO_2/SWNT coatings were rendered oleophobic by immersing substrate into 0.5 wt % 1*H*,1*H*,2*H*,2*H*-perfluorodecyltrichlorosilane (FDTS) (Indofine Chemical Co., U.S.) in hexane for 15 min. The samples were then rinsed in plain hexane to remove excess FDTS, dried using nitrogen, and cured at 120 °C in air for 1 h. To modulate the wettability of the coating, UV irradiation was carried out using a mercury lamp with wavelength of 365 nm and intensity of 21 mW/cm^2.

2.2. Characterization. The morphology of the TiO_2/SWNT coatings was investigated by a JEOL 6500 field-emission gun scanning electron microscope (SEM) at an accelerating voltage of 5 kV. Samples were not coated with an additional metal layer. The initially synthesized TiO_2/SWNT hybrid clusters were observed via a transmission electron microscope (TEM) (FEI Tecnai T12A) at an accelerating voltage of 120 kV. The TEM samples were gathered from the $(NH_4)_2TiF_6/H_3BO_3$ solution with dispersed SWNTs 5 min after reacting at 45 °C and centrifuged at 8000 rpm. The obtained precipitates were then ultrasonically dispersed in ethanol and transferred on 300 mesh copper grids with Formvar film by depositing a drop of the ethanol dispersion on the grids. The amount of FDTS on the coating surface at different UV illumination time was measured on an SSX-100 X-ray photoelectron spectroscopy (XPS) system (Surface Science Instruments) equipped with a monochromatized Al Kα X-ray source, a hemispherical sector analyzer, and a resistive anode detector. A metal grid above the samples as well as a low-energy electron flux (10 eV) were used for charge neutralization. The X-ray source was operated at 20 kV and 10 mA (200 W), and the spot size was 1 × 1 mm^2. Survey scan spectra were recorded at a pass energy of 150 eV and a step size of 1 eV, whereas individual high resolution spectra were taken at a pass energy of 50 eV with an energy step of 0.1 eV. The peak fittings were conducted using the ESCA 2005 software provided with the XPS system. Charge compensation was done by setting the C−H/C−C peak to 285.0 eV. A Gaussian−Lorentzian model with Gaussian percentages of 80−100% was applied to the peak fittings. X-ray diffraction (XRD) analysis of the composite coatings was carried out on a Bruker-AXS microdiffractometer with a 2.2 kW sealed Cu X-ray source.

Static contact angles for various liquids were measured using a contact angle meter, OCA15 Plus (Dataphysics Inc., Germany). For each sample, a minimum of five readings at different locations on the sample surface were recorded. The sliding angles were also measured using the same apparatus.

2.3. Fabrication of Smooth TiO_2 Films and Roughness Measurements. Smooth TiO_2 thin films were deposited on silicon wafer at 220 °C in a 200 mm diameter crossflow atomic layer deposition (ALD) reactor (Savannah S200, Cambridge NanoTech, U.S.). Using titanium tetraisopropoxide and water as precursors, the deposition proceeded for 300 loops, and finally anatase TiO_2 films with thickness around 20 nm were obtained.[23] Surface roughness of the ALD TiO_2 coatings was measured by using a Nanoscope III Multimode scanning probe microscope (Digital Instruments). The measurements were operated in tapping mode with a scan area of 1 × 1 μm^2. Final surface roughness was calculated by the average of 10 measurement points.

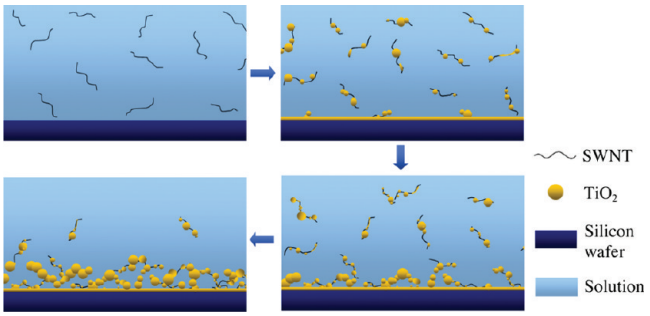

Figure 1. Illustration of the formation of overhanging structures in TiO_2/SWNT composite coatings.

3. RESULTS AND DISCUSSION

The nucleation and growth of the TiO_2 crystal caused by the hydrolysis of the metal fluoride complex mainly appears in the vicinity of the heterogeneous solid−liquid interface in the LPD process. When SWNTs were added in the reacting solution, the suspended nanotubes will be incorporated into TiO_2 as a result of the nucleation of TiO_2 crystals on the nanotube surface. Typical of surfaces with low coordination and interfacial energy, the nucleation of atoms on the carbon nanotube surface tends to form atom clusters rather than a continuous monolayer.[24,25] Therefore, TiO_2/SWNT hybrid clusters were formed in the solution. With the increase of TiO_2 particle size on SWNTs, the hybrid clusters settled down on the substrate and were gradually embedded in the coating (Figure 1). Finally, the overlapped TiO_2 clusters on the coating surface resulted in a highly porous coating with self-overhanging structures (Figure 2A−C). The TEM image of the TiO_2/SWNT hybrid clusters formed at the initial reaction stage is shown in Figure 2D.

The as-synthesized TiO_2/SWNT coatings demonstrate superhydrophilicity and strong capillary to water. XRD analysis shows that the synthesized TiO_2 crystals are in the anatase phase (Figure S1). When treated with FDTS to chemically lower the surface tension γ_{sv}, the composite coatings were changed from superhydrophilic to superoleophobic drastically, displaying a contact angle of 160.4° to silicone oil (γ_{lv} = 21.5 mN/m) with a sliding angle of 5.9° (Figure 2E).

A more detailed SEM observation reveals that the surface of the TiO_2 clusters is composed of nanocrystals with size of 30−50 nm (Figure 2B). Indeed, nanoscale TiO_2 particles generated at the initial stage of the LPD process (Figure 2D) are assembled together to form the TiO_2 clusters in microscale. The hierarchical surface structures therefore constructed are normally desired structures for a liquid-repellent surface, known as the lotus effect.[26]

When no SWNT was added in the solution, the obtained pure TiO_2 coatings showed a worse oil repellency with contact angles less than 140° to silicone oil. SEM observation shows that flake crystals were formed on the top of the TiO_2 clusters (Figure 3A,B).

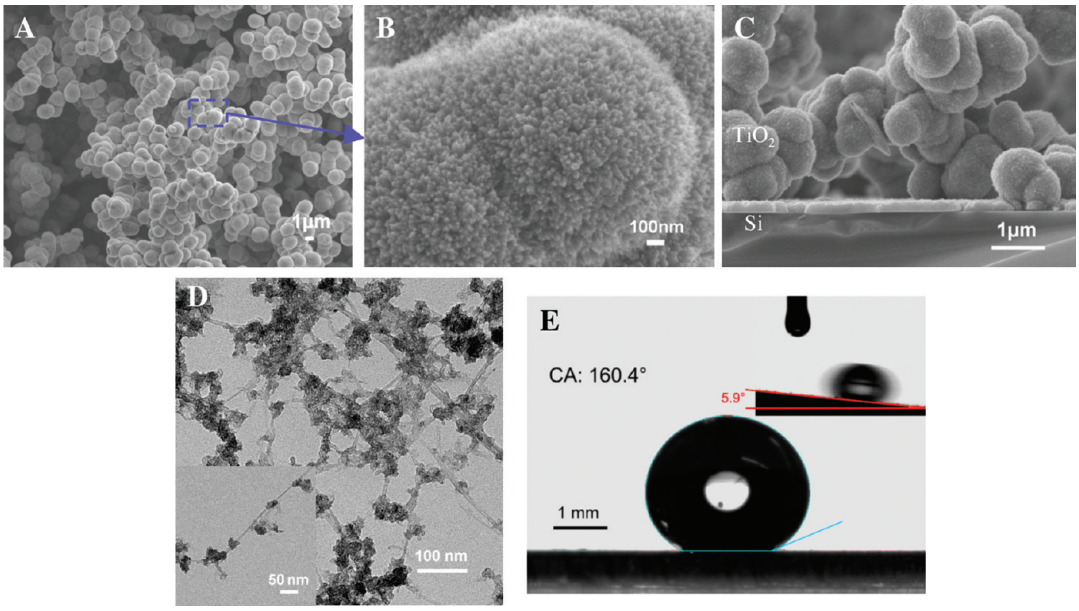

Figure 2. Superoleophobicity realized on a TiO_2/SWNT composite coating surface. (A) SEM images of the TiO_2/SWNT porous coating on a silicon wafer synthesized using 2 μg/mL SWNT. (B) The cross-section view of the coating shows overhanging structures formed by the TiO_2/SWNT clusters. (C) The high-magnification view of the coating surface shows that the surface of TiO_2 particles is covered by nanocrystals, forming hierarchical surface structures. (D) TEM image of the TiO_2/SWNT hybrid clusters synthesized at a reaction time of 5 min. The inset shows a single SWNT coated with TiO_2 clusters. (E) A droplet of silicone oil on top of the above coating. The inset shows a droplet of silicone oil rolling down a tilted coating surface.

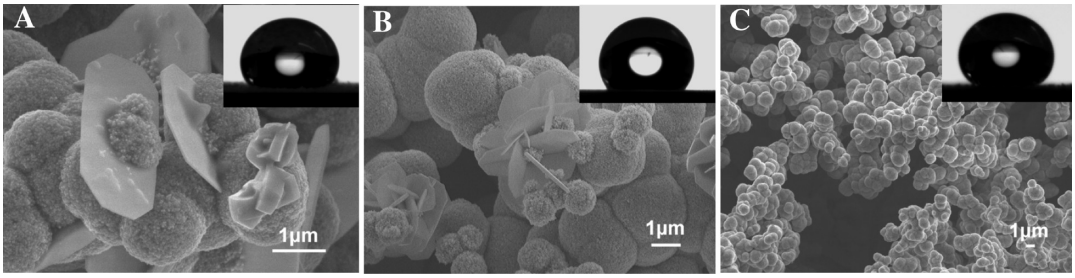

Figure 3. SEM images of TiO_2 coatings synthesized at SWNT concentrations of (A) 0, (B) 1, and (C) 4 μg/mL. The insets are drop shapes of silicone oil on the corresponding coating surface.

The flakes are ammonium oxotrifluorotitanate (NH_4TiOF_3) crystals grown together with TiO_2 particles probably due to the aggregation of the titanium fluoride complex in the vicinity of TiO_2 surface. The amount of NH_4TiOF_3 crystals in the coating decreased with the presence of SWNT in the solution and completely disappeared when the concentration of SWNT reached 2 μg/mL. When SWNTs were added, the solid−liquid interfaces in the reaction solution increased significantly due to the large specific surface area of the SWNT. The increased interface area facilitated the nucleation of TiO_2 crystals and decreased the average concentration of the titanium fluoride complex near the solid surfaces. Therefore, the nucleation rate of NH_4TiOF_3 is lowered. Moreover, during the growth of the NH_4TiOF_3 grains, the incorporation of SWNTs in the crystals can also inhibit their growth.

Improvement of the oil repellency was observed as the smooth and wettable NH_4TiOF_3 crystals were gradually removed from the coating surface. As shown in Figure 4, the contact angle of the composite coatings with silicone oil increased from 137° to 160° and the tilting angle decreased from 32° to 5.9° when the content

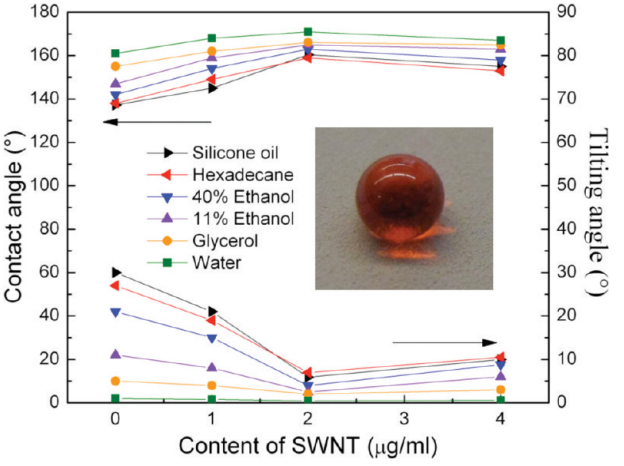

Figure 4. Contact angles and tilting angles for different liquids as a function of SWNT concentration. The inset shows a drop of silicone oil (dyed with Oil Red O) on a TiO_2/SWNT coating surface synthesized at SWNT concentration of 2 μg/mL.

dx.doi.org/10.1021/la200405b |*Langmuir* 2011, 27, 9295–9301

of SWNT in the reaction solution increased from 0 to 2 μg/mL. Further increasing the concentration of SWNT to 4 μg/mL caused a loose coating in which the TiO_2/SWNT hybrid clusters have little adhesion to each other (Figure 3C). This increases the instability of the Cassie state on the coating surface and thus degrades the oil repellent performance.

Under UV irradiation, TiO_2 surface can decompose the FDTS monolayer as a result of photocatalytic action. The decomposition process studied with XPS is shown in Figure 5. The atomic percentage of C−F bond (689.2 eV) in the F element decreased almost linearly with the UV illumination time and went down to zero after irradiation for 12 h, indicating that the FDTS on the coating surface can be completely decomposed. The XPS spectrum of TiO_2/SWNT coating without FDTS treatment was also presented for comparison. The peaks at 684.8 eV represent the TiF_6^- component, which probably comes from the trace of $(NH_4)_2TiF_6$ residues on the coating surface.

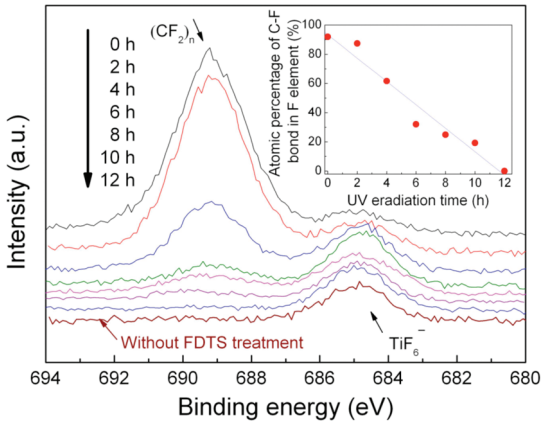

Figure 5. F 1s XPS spectra recorded on the FDTS-rendered TiO_2/SWNT coating surface under different UV irradiation time. The inset shows that the atomic percentage of C−F bond (corresponding to FDTS) varies with irradiation time, indicating the decomposition of FDTS under UV irradiation. The XPS spectrum of the TiO_2/SWNT coating without FDTS treatment is also presented for comparison.

Liquids with different surface tensions, hexadecane, 40% ethanol in water (γ_{lv} = 30.2 mN/m), 11.1% ethanol (γ_{lv} = 46.0 mN/m), glycerol, and water, were used to evaluate the wettability tuning effect of UV irradiation. As shown in Figure 6A, for each liquid, the contact angle of the coating decreased sharply and went to around zero when the irradiation time exceeded a critical value. This critical irradiation time is longer for liquids with higher surface tension. Eventually, after UV irradiation for 13 h, the coating was converted from superoleophobic to superhydrophilic. According to XPS results, one more hour of UV irradiation was needed to make the coating superhydrophilic after FDTS was completely decomposed. This might be because of some FDTS residues that underlie the TiO_2 overhanging structures and thus are hard to detect by XPS.

It is worth noting that during this conversion, the wettability of the coating can be tuned from superphobic to superphilic for every liquid tested. Moreover, by controlling the dose of the UV light, the same coating surface can be superphobic to one liquid while superphilic to another with lower surface tension. As shown in Figure 6A, before UV irradiation, the coating surface is superphobic to all of the liquids tested (corresponding to window I). At this time, both hexadecane and 40% ethanol (Figure 6B-I) can roll on the coating surface (Figure 6B-I, movie S1). After UV irradiation for 2 h, the coating was tuned from superoleophobic to superoleophilic with hexadecane due to the partial decomposition of FDTS. Meanwhile, the coating still remained superphobic to 40% ethanol and other liquids (window II). The two converse wetting states of hexadecane and 40% ethanol on the same coating were shown in Figure 6B-II (also movie S2). Given the small surface tension difference between hexadecane (27.6 mN/m) and 40% ethanol (30.2 mN/m), this method shows a capability to distinguish liquids with surface tension difference less than 5 mN/m.

By further increasing the illumination time, the same coating can be tuned to be superphobic and superphilic, respectively, for

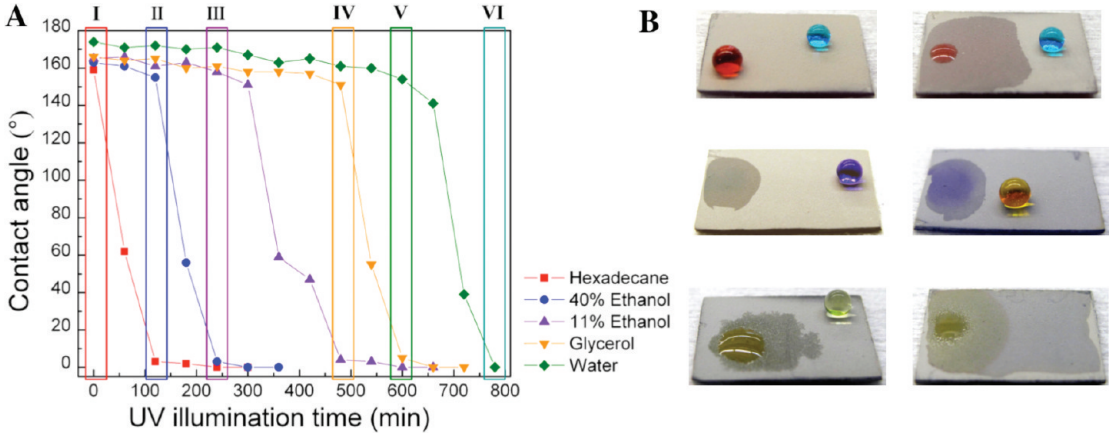

Figure 6. Wettability tuning of the TiO_2/SWNT coating using UV irradiation. (A) Contact angles (θ^*) for various liquids, including hexadecane, 40% ethanol, 11% ethanol, glycerol, and water as a function of UV irradiation time. Windows I−VI correspond to the surface states in which a liquid pair can be distinguished by complete converse wetting behavior on the coating surface. (B) Wetting behavior of liquid pairs on the coating with surface wetting states corresponding to windows I−VI in (A). I: Superphobic to both hexadecane (colored with Oil Red O) and 40% ethanol (dyed with methylene blue). II: Superphilic to hexadecane while superphobic to 40% ethanol. III: Superphilic to 40% ethanol while superphobic to 11% ethanol (dyed with methyl violet). IV: Superphilic to 11% ethanol while superphobic to glycerol (dyed with metanil yellow). V: Superphilic to glycerol while superphobic to water (methylene blue and metanil yellow were dissolved together in water to get a light green color). VI: Superphilic to both glycerol and water (also see movies S1−S6).

dx.doi.org/10.1021/la200405b |*Langmuir* 2011, 27, 9295–9301

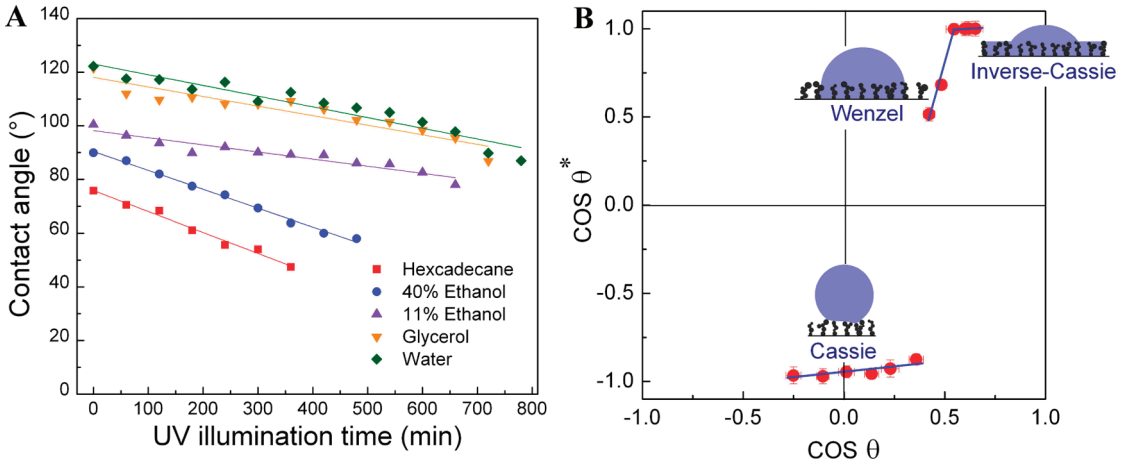

Figure 7. (A) Contact angles (θ) for various liquids, including hexadecane, 40% ethanol, 11% ethanol, glycerol, and water on smooth ALD TiO_2 surface as a function of UV irradiation time. θ decreased almost linearly with the irradiation time. (B) Plot of cos θ^* for 11% ethanol as a function of cos θ, showing the wetting state change with the decrease of θ. Blue lines are guides to the eye.

each pair of the liquids tested, including 40% ethanol versus 11% ethanol (46.0 mN/m) (Figure 6B-III), 11% ethanol versus glycerol (63.0 mN/m) (Figure 6-IV), and glycerol versus water (72.1 mN/m) (Figure 6B-V). Finally, with the FDTS decomposed completely after UV irradiation for 13 h, this porous coating was switched to superhydrophilic (Figure 6B-VI) and showed a strong capillary effect with water again.

To further understand the mechanism of this wettability tuning phenomenon, smooth anatase TiO_2 coatings were synthesized on silicon wafers using ALD and treated with FDTS. The coating thickness is about 20 nm, and the root-mean-square roughness is 0.4 nm. The contact angle changes of these smooth coatings to different liquids were recorded with increasing UV irradiation duration (Figure 7A) and compared to the corresponding rough c-LPD TiO_2/SWNT coatings. It is well-known that the relationship between wetting and roughness can be explained by two independently developed models, the Wenzel model[27] (eq 1) and the Cassie−Baxter model[19] (eq 2):

$$\cos\theta^* = r\cos\theta \quad (1)$$

$$\cos\theta^* = -1 + \phi_s(1 + \cos\theta) \quad (2)$$

where θ^* is the apparent contact angle on the textured surface, θ is the equilibrium contact angle on a smooth surface of the same material, r is the surface roughness, and ϕ_s is the fraction of the solid in contact with the liquid. Surfaces in Cassie state usually show superphobicity to liquids.

Figure 7B illustrates the plot of cos θ^* on the rough c-LPD coatings as a function of cos θ with respect to the smooth ALD coatings. (Only data for 11% ethanol are shown here for legible reading. The wetting diagram for other liquids can be found in Figure S2.) It is clear that the behavior of the liquids can be separated into three states with the decrease of θ. In the first state, the surface displays high apparent contact angles θ^* even when θ is smaller than 90° indicative of being in the Cassie state due to the presence of overhanging structures. The c-LPD coatings show a superphobic state to the liquids as a result of the trapping of air between liquid and surface textures. When θ is smaller than a critical value θ_c (about 69° for 11% ethanol), θ^* decreases rapidly from more than 150° to less than θ and keeps decreasing with θ.

Table 1. Values of ϕ_s, r, and ϕ_s' for Different Liquids

	hexadecane	40% ethanol	11% ethanol	glycerol	water
ϕ_s		0.121	0.091	0.079	0.061
r	2.43	2.06	1.62	1.61	1.45
ϕ_s'	0.010	0.018	0.024	0.033	

The slope of cos θ^* with respect to cos θ is larger than 1, indicating the wetting state falls into the Wenzel regime. A third linear regime with a slope much smaller than 1 was also observed when θ was further lowered to a second critical value θ_c'. In this regime, liquid penetrates inside the microtextures of the coating and surrounds the drop on which the contact angle is measured. Therefore, the liquid drop sits upon a mixture of solid and liquid. We refer to this hemiwicking/wicking state as the "inverse-Cassie" state, because it is the exact inversion of the Cassie state described above and can be expressed by:[28]

$$\cos\theta^* = 1 - \phi_s'(1 - \cos\theta) \quad (3)$$

where ϕ_s' is the fraction of the solid islands in the mixture area of solid and liquid. Superphilic surfaces are usually formed in this state.

The values of ϕ_s, r, and ϕ_s' for different liquids were calculated and are listed in Table 1. Interestingly, the three parameters vary with different liquids. ϕ_s increased from 0.061 to 0.121 with the decrease of liquid surface tension from 72.1 mN/m (water) to 30.2 mN/m (40% ethanol), indicating liquids with lower surface tension have larger solid−liquid contact area on the same coating surface when they are in the Cassie state. When in the inverse-Cassie state, on the contrary, liquids with lower surface tension have smaller solid−liquid contact area. In the inverse-Cassie state, a liquid drop sits on a composite surface consisting mainly of liquid, apart from a few solid islands. Low-surface-tension liquids more easily wet a solid surface, and, therefore, more solid surfaces are immersed in the liquid at the contact area, resulting in a smaller ϕ_s'. The roughness factor, r, defined as the ratio of true area of the solid surface to the apparent area, ranges from 1.45 to 2.43 when liquids go into the Wenzel state. Because of the nanoscale roughness formed by the nanostructures on the TiO_2

dx.doi.org/10.1021/la200405b |*Langmuir* 2011, 27, 9295–9301

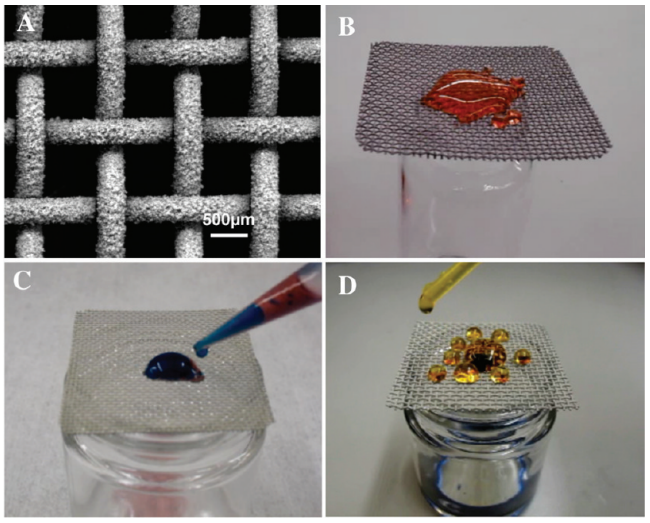

Figure 8. Liquids separation using a steel grid coated with TiO_2/SWNT composite coating. (A) Photo micrograph of the coated grid. (B) Silicone oil (dyed with Oil Red O) cannot pass through the grid without UV irradiation. (C) Mixture of silicone oil and 40% ethanol (colored with methylene blue) can be separated on the grid with UV irradiation for 2 h. (D) Separation of diiodomethane (colored with methyl violet) and glycerol (dyed with metanil yellow) on the same grid after UV irradiation for 7 h (see movies S7,S8).

surface, high-surface-tension liquids probably cannot get all of the true surface area wetted, resulting in a lower r.

From the above discussion, we can give a picture of the wettability tuning process on the composite coatings under UV irradiation. The coating surface changed from superphobic (Cassie state) to superphilic (inverse-Cassie state) rapidly through a middle wettable state (Wenzel state) as the intrinsic contact angle θ was reduced by UV irradiation. The critical irradiation time for this wettability jump increased with the increase of liquid surface tension, giving a time window (windows I–VI in Figure 6A) for a pair of liquids with different surface tensions. The coating surface shows both superphobic to one liquid and superphilic to the other in this window.

A useful application for this property is the separation of the mixture of liquids with different surface tensions. As shown in Figure 8, a stainless steel grid (square pores with 0.7 mm spacing) coated with the TiO_2/SWNT (Figure 8A) can be used to separate the mixture of silicone oil (21.5 mN/m) and 40% ethanol (30.2 mN/m) (Figure 8C, movie S7). Silicone oil droplets (red) can easily pass through the grid, whereas 40% ethanol (blue) mixed in the silicone oil beads up on the surface. No 40% ethanol was observed to go through the grid regardless of the size of the blue droplets in the mixture. By further increasing the surface energy of the coating to another level using UV irradiation, the same grid can also be used to separate diiodomethane (γ_{lv} = 50.8 mN/m) and glycerol (63.0 mN/m) (Figure 8D, movie S8). It is worth mentioning that, once tuned, the wettability of the composite coatings is quite stable with time. For example, the treated grid is still effective in liquid separation after being exposed in air for more than 90 days.

4. CONCLUSIONS

In summary, we have demonstrated that superoleophobic TiO_2/SWNT composite coatings can be obtained by a c-LPD method and the wettability of the coatings can be tuned from superphobic to superphilic with water and various organic liquids under UV irradiation. Liquids with surface tension difference smaller than 5 mN/m show completely inverse wetting states on the same modulated coating surface. On the basis of this property, the separation of organic liquids with different surface tensions on a TiO_2/SWNT coated grid was demonstrated. We anticipate that our approach may provide new pathways to microfluid control for not only water but also various liquids with lower surface tension.

■ ASSOCIATED CONTENT

Supporting Information. XRD pattern of TiO_2/SWNT coatings, complementary data of Figure 3D, corresponding videos for Figure 3C, and videos of liquids separation for silicone oil and 40% ethanol in water as well as diiodomethane and glycerol using TiO_2/SWNT-coated grid. This material is available free of charge via the Internet at http://pubs.acs.org.

■ AUTHOR INFORMATION

Corresponding Author
*E-mail: tcui@me.umn.edu.

■ ACKNOWLEDGMENT

The XRD, XPS, SEM, and TEM instruments were located in the University of Minnesota's open-access Characterization Facility, which is supported by operations funding from the Institute of Technology.

■ REFERENCES

(1) Gao, X.; Jiang, L. *Nature* **2004**, *432*, 36.
(2) Lee, W.; Jin, M. K.; Yoo, W. C.; Lee, J. K. *Langmuir* **2004**, *20*, 7665.
(3) Koch, K.; Barthlott, W. *Philos. Trans. R. Soc., A* **2009**, *367*, 1487.
(4) Erbil, H. Y.; Demirel, A. L.; Avci, Y.; Mert, O. *Science* **2003**, *299*, 1377.
(5) Wu, X.; Shi, G. *J. Phys. Chem. B* **2006**, *110*, 11247.
(6) (a) Wang, R.; Hashimoto, K.; Fujishima, A.; Chikuni, M.; Kojima, E.; Kitamura, A.; Shimohigoshi, M.; Watanabe, T. *Nature* **1997**, *388*, 431. (b) Liu, H.; Feng, L.; Zhai, J.; Jiang, L.; Zhu, D. *Langmuir* **2004**, *20*, 5659.
(7) Sun, T.; Wang, G.; Feng, L.; Liu, B.; Ma, Y.; Jiang, L.; Zhu, D. *Angew. Chem., Int. Ed.* **2004**, *43*, 357.
(8) Krupenkin, T. N.; Taylor, J. A.; Schneider, T. M.; Shu, Y. *Langmuir* **2004**, *20*, 3824.
(9) Chang, F.; Sheng, Y.; Chen, H.; Tsao, H. *Appl. Phys. Lett.* **2007**, *91*, 094108.
(10) Zhang, X.; Jin, M.; Liu, Z.; Tryk, D. A.; Nishimoto, S.; Murakami, T.; Fujishima, A. *J. Phys. Chem. C* **2007**, *111*, 14521.
(11) Tuteja, A.; Choi, W.; Ma, M.; Mabry, J. M.; Mazzella, S. A.; Rutledge, G. C.; Mckinley, G. H.; Cohen, R. E. *Science* **2007**, *318*, 1618.
(12) Steele, A.; Bayer, I.; Loth, E. *Nano Lett.* **2009**, *9*, 501.
(13) Wu, W.; Wang, X.; Wang, D.; Chen, M.; Zhou, F.; Liu, W.; Xue, Q. *Chem. Commun.* **2009**, *9*, 1043.
(14) Kumar, R. T. R.; Mogensen, K. B.; Bggild, P. *J. Phys. Chem. C* **2010**, *114*, 2936.
(15) Cao, L.; Price, T. P.; Weiss, M.; Gao, D. *Langmuir* **2008**, *24*, 1640.
(16) Zimmermann, J.; Rabe, M.; Artus, G. R. J.; Seeger, S. *Soft Matter* **2008**, *4*, 450.
(17) Leng, B.; Shao, Z.; de With, G.; Ming, W. *Langmuir* **2009**, *25*, 2456.

(18) Zhang, X.; Jin, M.; Liu, Z.; Nishimoto, S.; Saito, H.; Murakami, T.; Fujishima, A. *Langmuir* **2006**, *22*, 9477.
(19) Cassie, A. B. D.; Baxter, S. *Trans. Faraday Soc.* **1944**, *44*, 546.
(20) Deki, S.; Aoi, Y. *J. Mater. Res.* **1998**, *13*, 883–890.
(21) Deki, S.; Nakata, A.; Sakakibara, Y.; Mizuhata, M. *J. Phys. Chem. C* **2008**, *112*, 13535–13539.
(22) Lin, B.; Li, T.; Zhao, Y.; Huang, F.; Guo, L.; Feng, Y. *J. Chromatogr., A* **2008**, *1192*, 95.
(23) Pore, V.; Rahtu, A.; Leskelä, M.; Ritala, M.; Sajavaara, T.; Keinonen, J. *Chem. Vap. Deposition* **2004**, *10*, 143.
(24) Penner, R. M. *J. Phys. Chem. B* **2002**, *106*, 3339.
(25) Zoval, J. V.; Stiger, R. M.; Biernacki, P. R.; Penner, R. M. *J. Phys. Chem.* **1996**, *100*, 837.
(26) Barthlott, W.; Neinhuis, C. *Planta* **1997**, *202*, 1.
(27) Wenzel, R. N. *Ind. Eng. Chem.* **1936**, *28*, 988.
(28) Ishino, C.; Okumura, K. *Eur. Phys. J. E* **2008**, *25*, 415.